

Optimal Selection of Active Suspension Parameters Using Artificial Intelligence

M. Salehpour^{1,*}, A. Jamali² and N. Nariman-zadeh³

¹ P.h.D student, Islamic Azad University, Anzali branch, Anzali, Iran.

² Assistant professor, ³Professor, Faculty of Mechanical engineering, The University of Guilan, Rasht, Iran.

* m.salehpour@bandaranzaliiu.ac.ir

Abstract

In this paper, multi-objective uniform-diversity genetic algorithm (MUGA) with a diversity preserving mechanism called the ϵ -elimination algorithm is used for Pareto optimization of 5-degree of freedom vehicle vibration model considering the five conflicting functions simultaneously. The important conflicting objective functions that have been considered in this work are, namely, vertical acceleration of seat, vertical velocity of forward tire, vertical velocity of rear tire, relative displacement between sprung mass and forward tire and relative displacement between sprung mass and rear tire. Further, different pairs of these objective functions have also been selected for 2-objective optimization processes. The comparison of the obtained results with those in literature demonstrates the superiority of the results of this work. It is shown that the results of 5-objective optimization include those of 2-objective optimization and, therefore, provide more choices for optimal design of vehicle vibration model.

Keywords: Vehicle vibration model; Pareto; MUGA; Genetic algorithm; Multi-objective optimization

1. INTRODUCTION

Vibration control of machines worked by engines has attracted great amount of research activities during last decades. Particular, vehicles motions are influenced by the harmful effects of vibrations caused by engines and roads which have a pivotal role in driver's comfort. Griffin et al. [1], Rokheja [2] and Barak [3] have shown that the interior vibration of a vehicle have a significant effect in comfort and road holding capability. In some previous researches have been shown that the trade-off between comfort and road holding capability is difficult to achieve [4-6]. Today, there are three types of suspension system which are installed between road excitation and vehicle body and named passive suspension, active suspension and semi-active suspension. Passive suspension is composed of a parallel mounting of a spring and damper. This suspension type is commonly used by majority of manufacturers; but it can not compromise between road vehicle comfort and road holding capability, properly. Chalasani has shown that increasing of the passive suspension damping coefficient improves vehicle comfort but this improvement decreases road holding capability [7]. In case of reducing this limitation of passive suspension, the tendency of researchers has led them to produce

other kind of suspension system such as active suspension. Active suspension needs an external energy source. Moreover, it is capable of compromising between road vehicle comfort and road holding capability [8-11]. Thompson has presented that the result of using of active suspension is vibrantly superior to other types of suspension systems [12]. The other type of suspension is called semi-active. This type is halfway between the two other types, passive and active. The semi-active suspension creates an approximate active damping control law without the need of external energy source [13]. Bouazara in his PhD thesis studied three types of suspension system (active, semi-active and passive) for five and eight-degree of freedom vibration model [14]. In his works, Bouazara combined all the performance criteria to form an objective function for an optimization process. For this purpose, he used the weighting coefficients to adjust the comfort and road holding capability criteria in the single optimization design process. Further, he assign the vertical acceleration of seat as vehicle comfort and the relative displacement between sprung mass and tires as road holding capability. Using of weighing coefficients is not a proper approach to solve the multi-objective optimization problems. Because the results of the optimization are extremely depended on the weighing

coefficients and with the slight changing in the value of coefficients, the results would be different. Feng et al. adopted a combined control scheme for the vertical motion optimization of active vehicle suspension systems using a genetic algorithm based self-tuning PID controller and a fuzzy logic controller [15]. Alkhatib applied genetic algorithm (GA) method to the optimization problem of a linear one-degree of freedom (1-DOF) vibration isolator mount and the method was extended to the optimization of a linear quarter car suspension model [16]. The optimum solution was obtained numerically by utilizing GA and employing a cost function that sought minimizing absolute acceleration RMS (root mean square) sensitivity to changes in relative displacement RMS. Gündoğdu presented an optimization of a four-degree of freedom quarter car seat and suspension system using genetic algorithms to determine a set of parameters to achieve the best performance of the driver [17]. The desired objective was proposed as the minimization of a multi-objective function formed by the combination of not only suspension deflection and tire deflection but also the head acceleration and crest factor (CF), which is not practiced as usual by the designers. Nariman-zadeh et al. used a multi-objective approach for optimal design of a 5-degree of freedom vehicle vibration model with passive suspension [18]. In this reference, they obtained some Pareto fronts of non-dominated optimal design points of five non-commensurable objective functions, namely, vertical acceleration of seat, vertical velocities of forward and rear tires, relative displacements between sprung mass and both forward and rear tires.

In this paper, multi-objective uniform-diversity genetic algorithm (MUGA) with a diversity preserving mechanism called the $\hat{\alpha}$ -elimination algorithm is used for multi-objective optimization of a 5-degree of freedom vehicle vibration model. The conflicting objective functions that have been considered for minimization are, namely, vertical acceleration of seat (\ddot{z}_c), vertical velocity of forward tire (\dot{z}_1), vertical velocity of rear tire (\dot{z}_2), relative displacement between sprung mass and forward tire (d_1) and relative displacement between sprung mass and rear tire (d_2). The design variables used in the optimization of vibration are, namely, seat damping coefficient (c_{ss}), vehicle suspension damping coefficient (c_{s1} and c_{s2}), seat stiffness coefficient (k_{ss}), vehicle suspension stiffness coefficient (k_{s1} and k_{s2}),

damping coefficients for the active suspension (g_1 and g_2) and seat position in relation to the center of mass (r). Various pair-wise 2-objective optimization and 5-objective optimization processes are performed. The inclusion of the results by 5-objective optimization is verified using the results of different 2-objective optimization processes through some overlay graphs of the Pareto fronts. Prominently, it is shown that a trade-off optimum design can be verified from those Pareto fronts obtained by multi-objective optimization process. Finally, the superiority of time domain vibration performance of such design point is shown in comparison with those given in the literature.

2. MULTI-OBJECTIVE PARETO OPTIMIZATION

Multi-objective optimization that is also called multi-criteria optimization or vector optimization has been defined as finding a vector of decision variables satisfying constraints to give optimal values to all objective functions [21-22]. In general, it can be mathematically defined as:

find the vector $X^* = [x_1^*, x_2^*, \dots, x_n^*]^T$ to optimize

$$F(X) = [f_1(X), f_2(X), \dots, f_k(X)]^T, \quad (1)$$

subject to m inequality constraints

$$l_i(X) \leq 0 \quad , \quad i = 1 \text{ to } m, \quad (2)$$

and p equality constraints

$$h_j(X) = 0 \quad , \quad j = 1 \text{ to } p, \quad (3)$$

where, $X^* \in \mathfrak{R}^n$ is the vector of decision or design variables, and $F(X) \in \mathfrak{R}^k$ is the vector of objective functions. These objectives often conflict with each other so that improving one of them will deteriorate another. Therefore; there is no single optimal solution as the best with respect to all the objective functions. Instead, there is a set of optimal solutions, known as Pareto optimal solutions or Pareto front for multi-objective optimization problems [23-24].

Some unique natural properties of evolutionary algorithms like their parallel or population-based search scheme have been reasons to use them for multi-objective optimization problems. It should be noted that keeping the genetic diversity in the population or the Pareto front is one of the important

and main issue of these methods [21-22, 24-25]. The Pareto-based approach of NSGA-II [24] has been used in a wide range of engineering MOPs because of its simple yet efficient non-dominance ranking procedure in yielding different levels of Pareto frontiers. However, the crowding approach in such a state-of-the-art MOEA [25] works efficiently for two objective optimization problems as a diversity-preserving operator which is not the case for problems with more than two objective functions [18-20].

In this work, a recently reported multi-objective uniform-diversity genetic algorithm method called MUGA [18-20] is used for the multi-objective optimal design of vehicle vibration model. MUGA uses non-dominated sorting mechanism together with a ε -elimination diversity preserving algorithm to get Pareto optimal solutions of MOPs more precisely and uniformly. In fact, the basic idea of sorting of non-dominated solutions originally proposed by Goldberg [26] which has been used in different evolutionary multi-objective optimization algorithms, more importantly in NSGA II by Deb [24], has been adopted here. In order to improve the genetic diversity among the population, the ε -elimination diversity approach is used in which all the clones and ε -similar individuals are recognized and simply eliminated from population. Therefore, based on a value of ε as the elimination threshold, all the individuals in a front within this limit of a particular individual are eliminated. More detailed description of MUGA such as pseudo code of main algorithm, ε -elimination algorithm and etc., can be found in [18-20].

3. MULTI-OBJECTIVE OPTIMIZATION OF VEHICLE VIBRATION MODEL

A 5-degree of freedom vehicle with active suspension which is adopted from reference [14] is shown in Figure 1. This model is composed of one sprung mass that joints to three unsprung masses (indicate the tires and seat). Moreover, effect of degrees of freedom, linear motion (in vertical direction for sprung and unsprung masses), and rotating motion (pitching motion) for sprung mass, in terms of acceleration, velocity and movement, are exerted in formulation of motion equations. M_1 , m_2 , m_c , m_s , I_s , k_{p1} , k_{p2} , l_1 and l_2 which denote vehicle fixed parameters are expressed as forward tire mass, rear tire mass, seat mass, sprung mass, momentum inertia

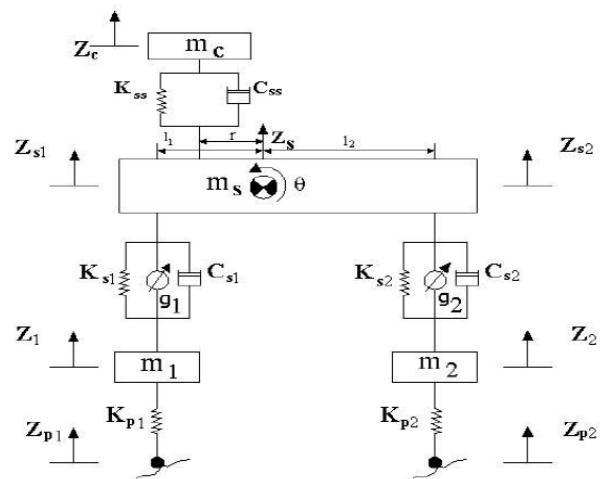


Fig. 1. Vehicle vibration five-degree of freedom model with active suspension adopted from reference [14]

of sprung mass, forward tire stiffness coefficient, rear tire stiffness coefficient, forward and rear suspensions position in relation to the center of mass, respectively. Design variables k_{ss} , k_{s1} and k_{s2} , c_{ss} , c_{s1} and c_{s2} , g_1 and g_2 and r denote seat stiffness coefficient, stiffness coefficients for vehicle suspension, seat damping coefficient, damping coefficients for vehicle suspension, damping coefficients for the active suspension and seat position in relation to the center of mass, respectively. g_1 and g_2 are the damping coefficients for the active suspensions obtained by the solution of Riccati equation [27]. Further, Subscripts 1 and 2 indicate tire axes, respectively. It is also necessary to observe that in this case study, seat type is composed of a linear spring and damper. This model is excited by a double-bump shown in figure 2.

The differential linearized equations of motion, with respect to the degrees of freedom and for small angle θ , are derived by the use of Newton-Euler equations and can be written as follows [14]:

$$z_{ps} = z_s - r\theta \quad (4)$$

$$z_{s1} = z_s - l_1\theta \quad (5)$$

$$z_{s2} = z_s + l_2\theta \quad (6)$$

$$F_{a1} = g_1\dot{z}_{s1} \quad (7)$$

$$F_{a2} = g_2\dot{z}_{s2} \quad (8)$$

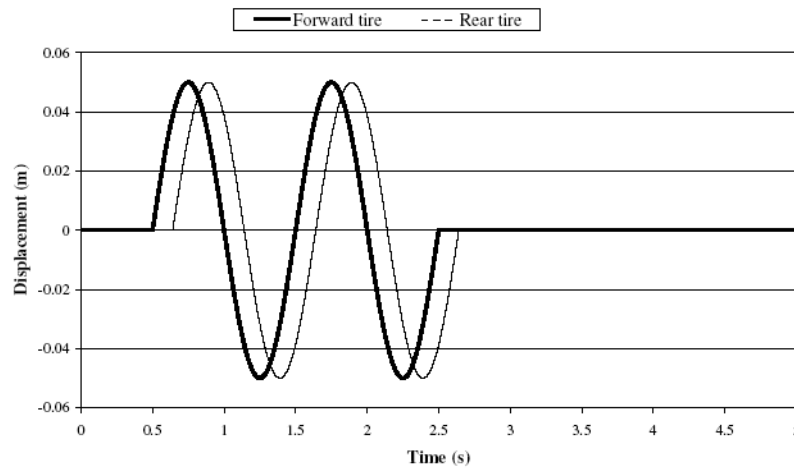


Fig. 2. Double bumps excitation

$$F_{ss} = k_{ss}(z_c - z_{ps}) + c_{ss}(\dot{z}_c - \dot{z}_{ps}) \quad (9)$$

$$F_{s1} = k_{s1}(z_{s1} - z_1) + c_{s1}(\dot{z}_{s1} - \dot{z}_1) \quad (10)$$

$$F_{s2} = k_{s2}(z_{s2} - z_2) + c_{s2}(\dot{z}_{s2} - \dot{z}_2) \quad (11)$$

$$m_c \ddot{z}_c = -F_{ss} \quad (12)$$

$$m_s \ddot{z}_s = -F_{s1} - F_{s2} + F_{ss} \quad (13)$$

$$I_s \ddot{\theta} = l_1 F_{s1} - l_2 F_{s2} - r F_{ss} \quad (14)$$

$$m_s \ddot{z}_{p1} = F_{s1} - k_{p1}(z_1 - z_{p1}) \quad (15)$$

$$m_s \ddot{z}_{p2} = F_{s2} - k_{p2}(z_2 - z_{p2}) \quad (16)$$

Where z_c , z_s , z_{si} and θ are vertical seat displacement, vertical displacement of the Central Gravity of the sprung mass, vertical displacement of the ends of the sprung mass and rotating motion (pitching motion), respectively. Further, \dot{z}_c , \dot{z}_i and \dot{z}_{si} represent vertical seat velocity, vertical tires velocity and vertical velocity of the ends of the sprung mass, respectively. \ddot{z}_c , \ddot{z}_s , \ddot{z}_i and $\ddot{\theta}$ denote vertical seat acceleration, vertical acceleration of the Central Gravity of the sprung mass, vertical tires acceleration and rotating acceleration (pitch acceleration), respectively. The damping force generated is given as follow [14]:

$$F_{aj} = g_j \dot{z}_{sj} \quad (17)$$

Lastly, z_{p1} and z_{p2} represent the excitation via road double bumps, as shown in figure 2.

It is supposed that the vehicle moves at constant velocity $v=20$ m/s over double bump, and it is further assumed that the rear tire follows the same trajectory as the front tire with a delay of $\Delta t = (l_f + l_v)/v$. The input values of fixed parameters are presented at Table 1 [14].

In this paper, $50000 < k_{ss}(\text{N/m}) < 150000$, $10000 < k_{s1}(\text{N/m}) < 20000$, $10000 < k_{s2}(\text{N/m}) < 20000$, $1000 < c_{ss}(\text{Ns/m}) < 4000$, $500 < c_{s1}(\text{Ns/m}) < 2000$, $500 < c_{s2}(\text{Ns/m}) < 2000$, $500 < g_{I, g_I}(\text{Ns/m}) < 2000$ and $0 < r < 0.5$ are observed as design variables to be

Table 1. The input values of fixed parameters of this paper

l_1	1.011 m
l_2	1.803 m
m_1	40 kg
m_2	35.5 kg
m_c	75 kg
m_s	730 kg
I_s	1230 kg.m ²
k_{p1}	175500 N /m
k_{p2}	175500 N /m

optimally found based on multi-objective optimization of 5 different objective functions, namely, vertical acceleration of seat (\ddot{z}_c), vertical velocity of forward tire (\dot{z}_1), vertical velocity of rear tire (\dot{z}_2), relative displacement between sprung mass and forward tire (d_1) and relative displacement between sprung mass and rear tire (d_2).

4. TWO-OBJECTIVE OPTIMIZATION OF VEHICLE VIBRATION MODEL

In this section, MUGA is used for multi-objective design of vehicle model which has been shown in Figure 1. For this purpose, five different pairs out of ten possible pairs of objectives are considered in bi-objective optimization processes. Such pairs of objectives to be optimized separately have been chosen as (\ddot{z}_c, \dot{z}_1) , (\ddot{z}_c, \dot{z}_2) , (\ddot{z}_c, d_1) , (\ddot{z}_c, d_2) and (d_1, d_2) which stands for vertical acceleration of seat with vertical velocity of forward tire, vertical velocity of rear tire, relative displacement between sprung mass and forward tire, and relative displacement between sprung mass and rear tire and relative displacement between sprung mass and forward tire with relative displacement between sprung mass and rear tire, respectively. Evidently, it can be observed that all of the objective functions are minimized in those sets of objective functions. A population of 80 individuals with a crossover probability of 0.9 and mutation probability of 0.1 has been used in 240 generations. Pareto fronts of each chosen pair of two objectives

have been shown through figures 3-7. It is clear from all of the figures that obtaining a better value of one objective would normally cause a worse value of another objective. However, if the set of decision variables is selected based on each of a Pareto front, it will lead to the best possible combination of that pair of objectives. In other words, if any other set of decision variables is chosen, the corresponding values of pair of objectives will locate a point inferior to the corresponding Pareto front. Such inferior area in the space of the objective functions for figures 3-7 are in fact top/right sides.

Figure 3 depicts the Pareto front of vertical acceleration of seat and vertical velocity of forward tire representing different non-dominated optimum points with respect to the conflicting objectives. In this figure, points A and C stand for the best vertical acceleration of seat and the best vertical velocity of forward tire, respectively. It should be noted that all the optimum design points in this Pareto fronts are non-dominated and could be chosen by a designer. It is clear from this figure that choosing a better value for any objective function in these Pareto fronts would cause a worse value of another objective function. Clearly, there are some important optimal design facts between these objective functions that can readily be observed in that Pareto front. Such important design facts could not have been found without the use of Pareto optimization approach of vehicle vibration model. In figure 3, point B₁ is the point which demonstrates an important optimal design fact.

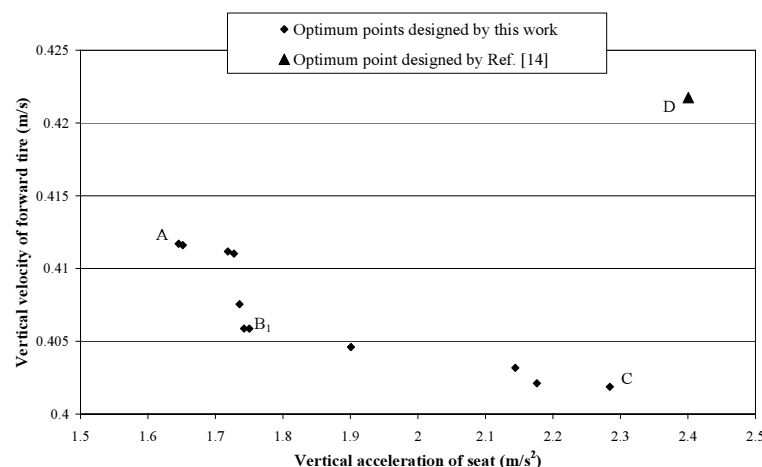


Fig. 3. Pareto front for vertical acceleration of seat and vertical velocity of forward tire in 2-objective optimization

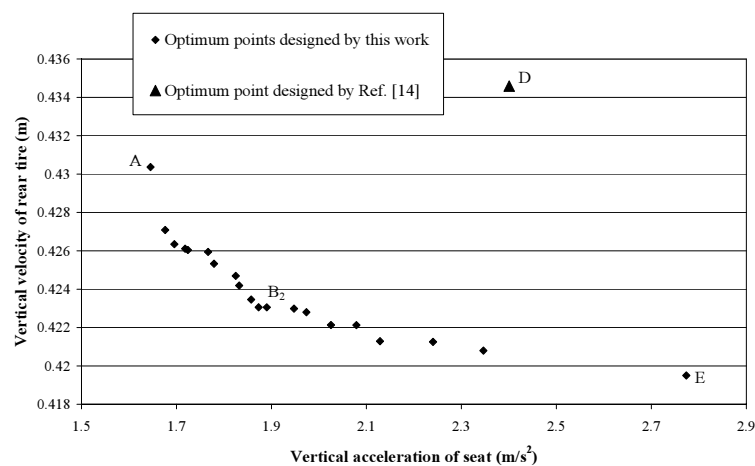


Fig. 4. Pareto front for vertical acceleration of seat and vertical velocity of rear tire in 2-objective optimization

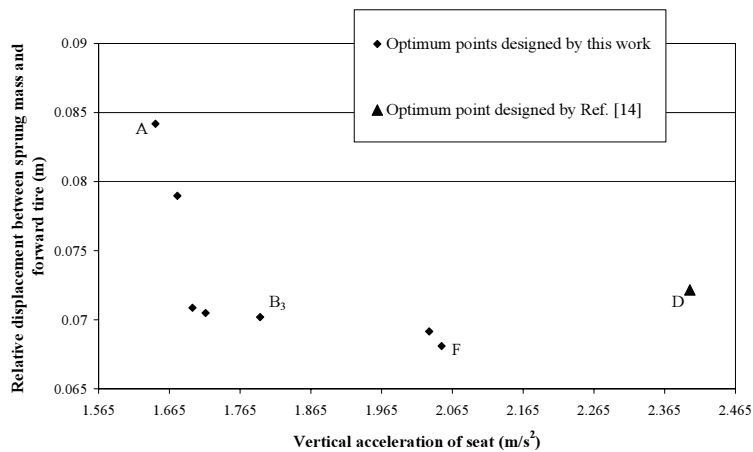


Fig. 5. Pareto front for vertical acceleration of seat and relative displacement between sprung mass and forward tire in 2-objective optimization

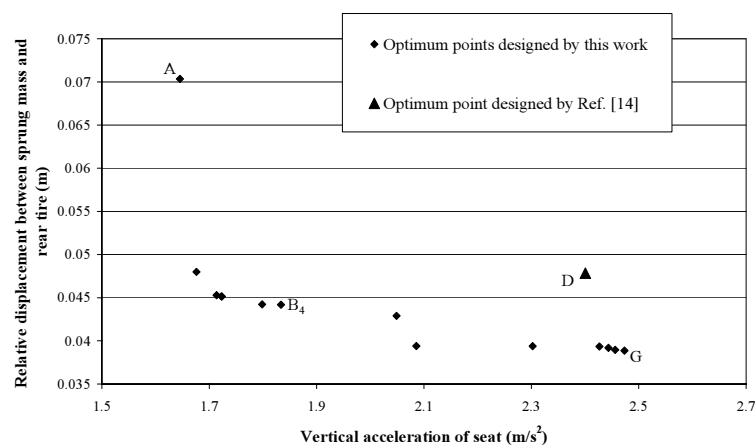


Fig. 6. Pareto front for vertical acceleration of seat and relative displacement between sprung mass and rear tire in 2-objective optimization

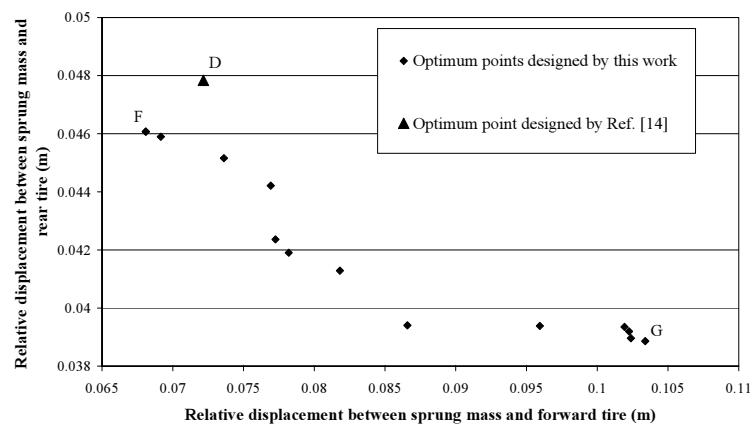


Fig. 7. Pareto front for relative displacement between sprung mass and forward tire and relative displacement between sprung mass and rear tire in 2-objective optimization

Optimum design point B_1 obtained in this paper exhibits a small increase in forward tire velocity in comparison with that of point C (the design with the least vertical velocity of forward tire) whilst its vertical seat acceleration improves about 23%. In fact, trade-off design point, B_1 , would not have been obtained without the use of the Pareto optimum approach presented in this paper.

Such non-dominated Pareto fronts of the other chosen sets of objective functions have been shown through figures 4-7. As considered in these figures, point A stands for the best vertical acceleration of seat whilst points E, F and G represent the best \dot{z}_2 , d_1 and d_2 , respectively. Similarly, the trade-off designing points B_2 , B_3 and B_4 are the design points which

demonstrate the important optimal design fact. With more careful observation, it is found that the values of seat accelerations improve about 32%, 13% and 26% with a small increase in other objective functions from points E to B_2 , F to B_3 and G to B_4 in figures 4, 5 and 6, respectively. In all these figures, point D represents the optimum design obtained in reference [14] which it is very evident that is vigorously dominated by all Pareto fronts shown in these figures. It is necessary to observe that in figure 7 point F represents optimum point from both two objective functions, and further shows less values comparing to point D.

The corresponding values of objective functions and design variables of these optimum design points and the point one in reference [14] are given in Table 2.

Table 2. The values of objective functions and their associated design variables of the optimum points of this work and the one of reference [14]

	A	B_1	C	B_2	E	B_3	F	B_4	G	H	D
k_{ss} (N/m)	150000	105555.6	57936.51	146825.4	116666.7	146825.4	123015.9	137301.6	137301.6	146825.4	105626
C_{ss} (Ns/m)	3047.619	3571.429	3333.333	3285.714	1047.619	3809.524	3857.143	2380.952	2380.952	3238.095	2666
k_{s1} (N/m)	10793.65	11111.11	16190.48	11428.57	18730.16	11428.57	10317.46	10000	10000	11111.11	15016
C_{s1} (Ns/m)	1023.81	1071.429	1238.095	738.0952	619.0476	1785.714	1976.19	785.7143	619.0476	1238.095	1942
k_{s2} (N/m)	10793.65	10000	10317.46	10000	10000	10634.92	15079.37	10000	19047.62	10000	15065
C_{s2} (Ns/m)	714.2857	666.6667	880.9524	1071.429	1714.286	1928.571	2000	2000	1976.19	1666.667	1954
r (m)	0.396827	0.341273	0.357146	0.333337	0.3254	0.293655	0.198419	0.2381	0.428573	0.396827	0.279
g_1 (Ns/m)	1761.905	880.9524	523.8095	880.9524	738.0952	1714.286	1952.381	1761.905	595.2381	1428.571	1674
g_2 (Ns/m)	1976.19	2000	1976.19	1976.19	1976.19	1928.571	1476.19	1619.048	1857.143	2000	1366
\ddot{z}_c (m/s^2)	1.645373	1.750178	2.284365	1.890136	2.773651	1.793258	2.049758	1.833712	2.473406	1.766512	2.400613
\dot{z}_1 (m/s)	0.411704	0.405873	0.401874	0.409386	0.407294	0.417264	0.423294	0.418934	0.41451	0.412741	0.421748
\dot{z}_2 (m/s)	0.430368	0.428452	0.422589	0.423056	0.419502	0.429314	0.43597	0.427993	0.429991	0.425943	0.434588
d_1 (m)	0.084189	0.089349	0.091624	0.093436	0.09824	0.070194	0.068094	0.082494	0.103389	0.078278	0.072163
d_2 (m)	0.070351	0.0736	0.075207	0.061469	0.057904	0.049523	0.046073	0.044187	0.038863	0.051928	0.047842

The Pareto optimum approach of this paper reveals some interesting and informative design aspects that may not have been found without multi-objective optimization. However, all such important and worthy information regarding the trade-off design point can also be simply discovered using a five-objective Pareto optimization instead of five separate bi-objective optimization processes.

5. FIVE-OBJECTIVE OPTIMIZATION OF VEHICLE VIBRATION MODEL

A multi-objective optimization design of vehicle model including all five objectives simultaneously can offer more choices for a designer. Moreover, such 5-objective optimization can subsume all the 2-objective optimization results presented in the previous section. This will allow finding a trade-off optimum design points from the view of all five objective functions simultaneously. Therefore, in this section, five objective functions, namely, vertical acceleration of seat (\ddot{z}_c), vertical velocity of forward tire (\dot{z}_1), vertical velocity of rear tire (\dot{z}_2), relative displacement between sprung mass and forward tire (d_1) and relative displacement between sprung mass and rear tire (d_2) are chosen for multi-objective optimization in which all of them are minimized simultaneously. A population of 80 individuals with a crossover probability of 0.9 and mutation probability of 0.1 has been used in 240 generations.

Figure 8 depicts the non-dominated individuals of 5-

objective optimization in the plane of ($\ddot{z}_c - \dot{z}_1$) together with the results to 2-objective optimization found in previous section. Such non-dominated individuals of both 5 and 2-objective optimization have alternatively been shown in the plane of ($\ddot{z}_c - \dot{z}_2$), ($\ddot{z}_c - d_1$), ($\ddot{z}_c - d_2$) and ($d_1 - d_2$) through figures 9-12, respectively. It should be noted that there is a single set of individuals as a result of 5-objective optimization of \ddot{z}_c , \dot{z}_1 , \dot{z}_2 , d_1 and d_2 that are shown in different planes together with the corresponding 2-objective optimization results. Therefore, there are some points in each plane that may dominate others in the case of 5-objective optimization. However, these individuals are all non-dominated when considering all five objectives simultaneously. By careful investigation of the results of 5-objective optimization in each plane, the Pareto fronts of the corresponding two-objective optimization previously found can now be observed in these figures. It can readily be observed that the results of such 5-objective optimization include the Pareto fronts of each 2-objective optimization and provide, therefore, more optimal choices for the designer.

It is now desired to obtain an optimum design point out of all non-dominated 5-objective optimization process somehow satisfying all five objective functions. In other words, each of the obtained design points given in previous section is acceptable based on pertinent two objective functions, but there is no reason that such an optimum design point existed in one of the Pareto fronts (i.e. plane of ($\ddot{z}_c - \dot{z}_1$)) is located in the other Pareto fronts too (i.e. plane of ($\ddot{z}_c - \dot{z}_2$)).

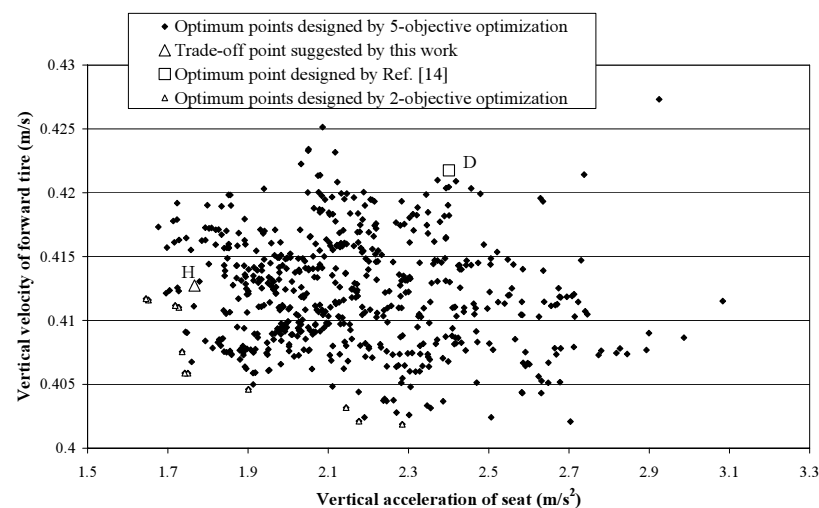


Fig. 8. Vertical acceleration of seat with vertical velocity of forward tire in both 5-objective & 2-objective optimization.

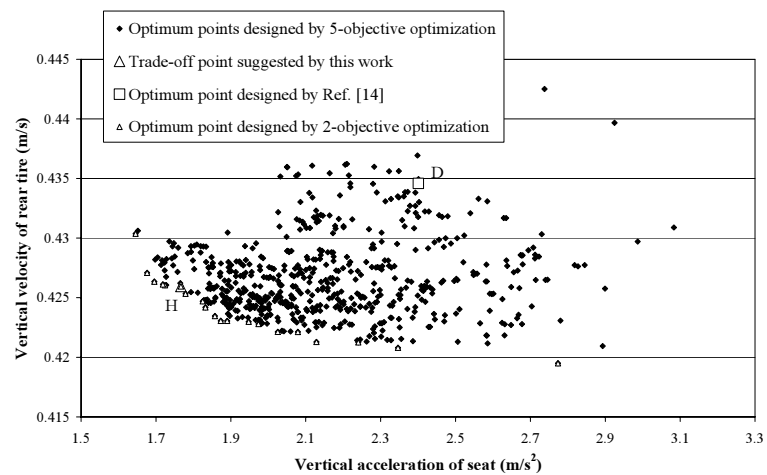


Fig. 9. Vertical acceleration of seat with vertical velocity of rear tire in both 5-objective & 2-objective optimization

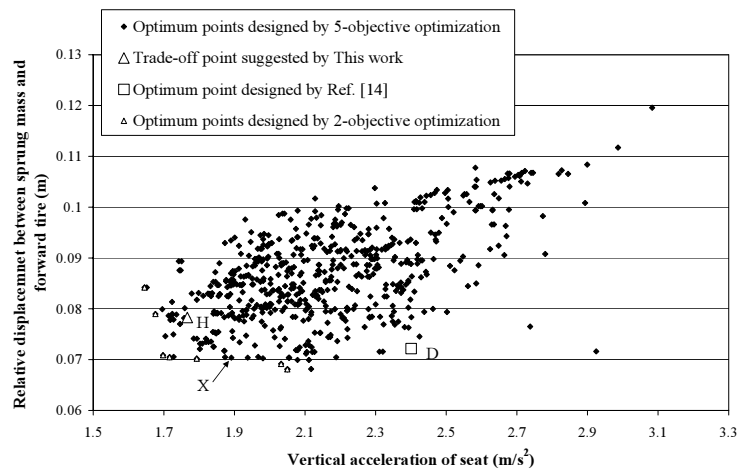


Fig. 10. Vertical acceleration of seat with relative displacement between sprung mass and forward tire in both 5-objective & 2-objective optimization

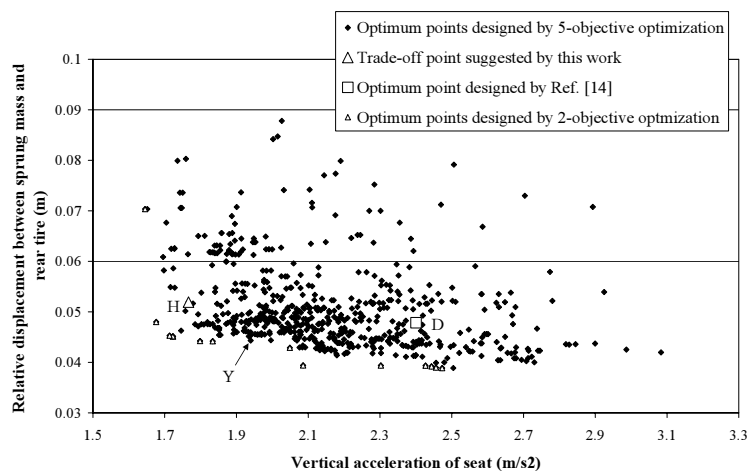


Fig. 11. Vertical acceleration of seat with relative displacement between sprung mass and rear tire in both 5-objective & 2-objective optimization

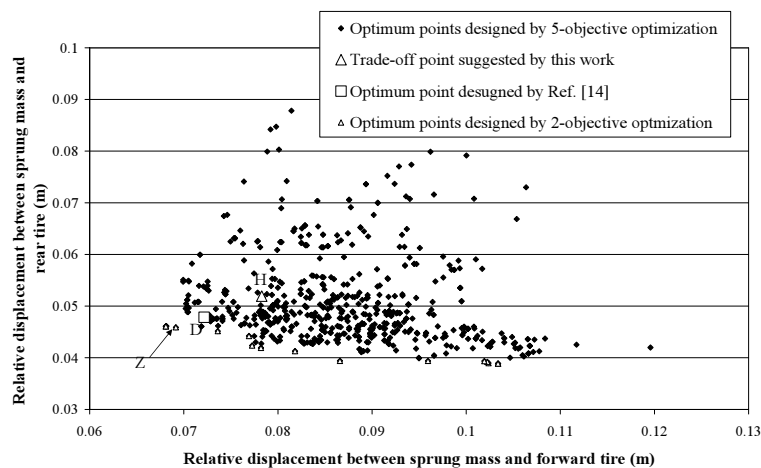


Fig. 12. Relative displacement between sprung mass and forward tire with relative displacement between sprung mass and rear tire in both 5-objective & 2-objective optimization

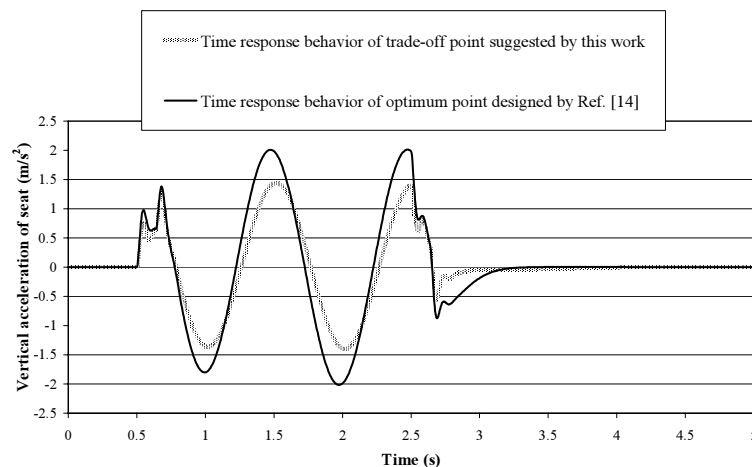


Fig. 13. Comparison of time response behavior of vertical acceleration of seat between points H, D

It is now possible to seek an optimum design point which is located almost on all Pareto fronts of figures 8 through 12. This can be simply achieved by mapping of the values of objective functions of all non-dominated points into interval 0 and 1. Using the sum of these values for each non-dominated points, the design point H simply represents the minimum of those values. It can be seen that the design point H located on all Pareto fronts approximately. Moreover, it can be seen that in two planes ($(\ddot{z}_c - \dot{z}_1)$ and $(\ddot{z}_c - \dot{z}_2)$) point H dominates point D proposed by reference [14]; in two planes ($(\ddot{z}_c - d_1)$ and $(\ddot{z}_c - d_2)$), no one dominates together and only in the last plane, point D dominates point H. But with a careful observation, it could be inferred that there are several optimum points designed by 2 & 5-objective optimization in these

three planes that dominate point D (i.e. points X, Y and Z in figures 10 through 12).

It should be noted that time response behavior of vertical acceleration of seat of proposed optimum point of this work and the one of reference [14] of vertical acceleration of seat are shown in figure 13. It is clear that time response behavior of point H is superior to that of point D. The values of objective functions and their associated design variables of H are shown in Table 2. The comparison of the values of objective functions associated with the optimum point H obtained from 5-objective functions optimization with those of 2-objective functions optimization of design points B_1 , B_2 , B_3 , B_4 and F given in Table 2 demonstrates the relative superiority of design point H.

Therefore, such multi-objective optimization of

vertical acceleration of seat (\ddot{z}_c), vertical velocity of forward tire (\dot{z}_1), vertical velocity of rear tire (\dot{z}_2), relative displacement between sprung mass and forward tire (d_1) and relative displacement between sprung mass and rear tire (d_2) provide optimal choices of design variables based on Pareto non-dominated points.

6. CONCLUSION

A multi-objective uniform-diversity genetic algorithm (MUGA) with a diversity preserving ability was used to optimally design of vehicle vibration model. The objective functions which conflict with each other were selected as vertical acceleration of seat (\ddot{z}_c), vertical velocity of forward tire (\dot{z}_1), vertical velocity of rear tire (\dot{z}_2), relative displacement between sprung mass and forward tire (d_1) and relative displacement between sprung mass and rear tire (d_2). The multi-objective optimization of vehicle model led to the discovering some important trade-offs among those objective functions. The superiority of the obtained optimum design points was shown in comparison with those reported in literature. Such multi-objective optimization of vehicle model could unveil very important design trade-offs between conflicting objective functions which would not have been found otherwise. Further, it has been shown that the results of 5-objective optimization include those of 2-objective optimization in terms of Pareto frontiers and provide, consequently, more choices for optimal design.

REFERENCES

- [1]. Griffin, M., Parsons, K., Whitham, E., 1982. Vibration and comfort. IV. Application of experimental results. *Ergonomics* 25, 721–739.
- [2]. Rakheja, S., 1985. Computer-aided Dynamic Analysis and Optimal Design of Suspension Systems for Off-road Tractors. PhD Thesis. Concordia University, Canada.
- [3]. Barak, P., 1991. Magic numbers in design of suspensions for passenger cars. Passenger Car Meeting, Tennessee, SAE Paper 911921, pp. 53–88.
- [4]. Karnopp, D., 1989. Analytical results for optimum actively damped suspensions under random excitation. *ASME Journal of Vibration, Acoustics, Stress, and Reliability in Design* 111 (July), 278–283.
- [5]. Hac, A., Youn, I., 1992. Optimal semi-active suspension with preview based on a quarter car model. *ASME Journal of Vibration and Acoustics* 114, 84–92.
- [6]. Bauml, A.E., McPhee, J.J., Calamai, P.H., 1996. Genetic algorithm optimization for active vehicle suspension design, in: CSME Congress, pp. 455–464.
- [7]. Chalasani, R.M., 1986. Ride performance potential of active suspension systems part 1: Simplified analysis based on a quarter-car model, in: Symposium on Simulation and Control of Ground Vehicles and Transportation Systems AMD-80 (DSC.2), pp. 187–204.
- [8]. Bouazara, M., Richard, M.J., 1996. An optimal design method to control the vibrations of suspensions for passenger cars, in: International Mechanical Engineering Congress and Exposition: The Winter Annual Meeting of ASME, Atlanta, DSC 58, pp. 61–68.
- [9]. Hrovat, D., 1991, Optimal active suspensions for 3d vehicle models. In: Proceedings of the American Control Conference, vol. 2, Arizona, USA, pp. 1534–1541.
- [10]. Goodall, R.M., Kortüm, W., 1983. Active control in ground transportation – a review of the state-of-the-art and future potential. *Vehicle System Dynamics* 12, 225–257.
- [11]. Yi, K., Hedrick, J.K., 1992. The use of semi-active suspensions to reduce pavement damage, in: Henry, J.J., Wamblod, J.C. (Eds.), *Vehicle, Tire, Pavement Interface*, ASTM STP 1164, American Society for Testing and Materials, Philadelphia, pp. 1–13.
- [12]. Thompson, A.G., 1989. The effect of tire damping on the performance of vibration absorbers in an active suspension. *ASME Journal of Sound and Vibration* 133 (3), 457–465.
- [13]. Redfield, R.C., 1991. Performance of low-bandwidth, semi-active damping concept for suspension control. *Vehicle System Dynamics* 20, 245–267.
- [14]. Bouazara, M., 1997. Etude et Analyse de la Suspension Active et Semi-active des Vehicules Routiers. Ph.D. Thesis, Université Laval, Canada.

- [15]. Feng, J. Z., LI, J., and YU, F., 2003. GA-based PID and Fuzzy Logic control for active vehicle suspension system. *International Journal of Automotive Technology* 4 (4), 181-191.
- [16]. Alkhatib, R., Nakhaie Jazar, G., Golnaraghi, M.F., 2004. Optimal design of passive linear suspension using genetic algorithm. *Journal of Sound and Vibration* 275, 665–691.
- [17]. Ö. Gündoğdu, 2007. Optimal seat and suspension design for a quarter car with driver model using genetic algorithms, *International Journal of Industrial Ergonomics* 37 (4), 327-332.
- [18]. Nariman-Zadeh, N., Salehpour, M., Jamali, A., Haghgoo, E., 2010. Pareto optimization of a five-degree of freedom vehicle vibration model using a multi-objective uniform-diversity genetic algorithm (MUGA). *Engineering Applications of Artificial Intelligence* 23(4), 543-551, 2010.
- [19]. Jamali, A., Nariman-Zadeh, N., Atashkari, K., 2008. Multi-objective Uniform diversity Genetic Algorithm (MUGA), In *Advanced in Evolutionary Algorithms*, witold kosinski (Ed.), IN-TECH, Vienna.
- [20]. Jamali, A., Hajiloo, A., Nariman-zadeh, N., 2010. Reliability-based robust Pareto design of linear state feedback controllers using a multi-objective uniform- diversity genetic algorithm (MUGA). *Expert Systems with Applications* 37 (1), 401–413.
- [21]. Nariman-Zadeh, N., Atashkari, K., Jamali, A., Pilechi, A., Yao, X., 2005. Inverse modeling of multi-objective thermodynamically optimized turbojet engine using GMDH-type neural networks and evolutionary algorithms. *Engineering Optimization* 37 (26), 437–462.
- [22]. Coello Coello, C.A., Becerra, R.L., 2003. Evolutionary multi-objective optimization using a cultural algorithm. In: *Swarm, IEEE (Ed.), Intelligence Symposium*, IEEE Service Center, Piscataway, pp. 6–13.
- [23]. Diwekar, U.M., Kalagnaman, J.R., 1997. Efficient sampling technique for optimization under uncertainty. *American Institute of Chemical Engineering Journal* 43 (2) 440-447.
- [24]. Deb, K., Agrawal, S., Pratap, A., Meyarivan, T., 2002. A fast and elitist multi- objective genetic algorithm: NSGA-II. *IEEE Transactions on Evolutionary Computation* 6 (2), 182–197.
- [25]. Coello Coello, C.A., Van Veldhuizen, D.A., Lamont, G.B., 2002. In: *Evolutionary Algorithms for Solving Multi-Objective Problems*. Kluwer Academic, Dordrecht.
- [26]. Goldberg, D.E., 1989. *Genetic algorithms in search, Optimization, and Machine Learning*. Addison-Wesley, Reading, MA.
- [27]. Bouazara, M., 1991. L'influence des paramètres de suspension sur le comportement d'un véhicule. Master's thesis. Université Laval, Canada.